A new type of sea bed waves

Michiel A.F. Knaapen, Suzanne J.M.H. Hulscher, Huib J. de Vriend

Departement of Civil Engineering, University of Twente

Ad Stolk

Netherlands Ministry of Transport, Public Works and Water Management, North Sea Directorate

Abstract. Sandy beds of shallow tidal seas often exhibit a range of rhythmic patterns, from small-scale ripples a few metres long to large tidal sandbanks with a wavelength of kilometres. For example, on the access route to Rotterdam harbour ships cross a field of sandwaves. The crests of these sandwaves determine the effective navigation depth. To warrant navigability, the North Sea Directorate of the Netherlands Ministry of Transport, Public Works and Water Management continually monitors the bathymetry in the sandwave area, originally using echo sounding. Our analysis of these data has revealed a new rhythmic pattern, in addition to the well-known sandwaves and tidal sandbanks. The wavelength of this new pattern, labelled here as long bedwaves, is three times the one of sandwaves, and the crest orientation is different. Interference of the three modes leads to the rather complex bathymetry revealed by echo soundings.

Seabed topography

Tidal sandbanks (wavelength 5-10 km, height up to the water depth) are the largest rhythmic features in shallow shelf seas with a sandy bed [*Off*, 1963]. They can be explained as manifestations of the unstable interaction between the depth-averaged tidal current, the attending sediment transport and morphological changes due to the horizontal divergence of the flow field [*Hulscher*, 1996; *Huthnance*, 1982]. Other scientists find that the location of tidal sandbanks is not only controlled by hydrodynamic conditions, but also by the presence of older morphological features. These features act as a core for tidal sandbank growth [*Pattiaratchi and Collins*, 1987; *Trentesaux et al.*, 1999].

Sandwaves (wavelength 500-800 m, amplitude up to 10% of the water depth) are generally considered the next smaller-scale pattern. Sandwaves can be explained from the unstable interaction in the vertical between tidal currents, sediment transport and morphological changes [*Komarova and Hulscher*, 2000; *Hulscher*, 1996]. Sandwaves reduce the navigation depth and are a threat to submarine pipelines and cables [*Meijdam and Lapidaire*, 1995].

Note that the classification is based on the physical generation mechanism. Geologists classify seabed waves based on the internal structure. To them, sandwaves are large dunes, sandbanks are ridges.

Paper number 1999GL000000.
0094-8276/01/1999GL000000$05.00

Measurements

In the Noordhinder area, at the offshore end of the access channel to Rotterdam Harbour halfway between the Netherlands and England, detailed bathymetric surveys have been made by the North Sea Directorate of the Netherlands Ministry of Transport, Public Works and Water Management (Figure 1) [*van Maren*, 1998]. Echo sounders determine the distance from ship to seabed from the travelling time of a sound signal, taking into account the density of the water. The depth values are corrected for the instantaneous vertical tide. The 1990 bathymetric data discussed in this article were taken using a single beam Atlas Deso 20 echosounder with a frequency of 210 kHz. The measuring tracks were 50 m apart. Along the tracks, every 5 m a water depth was recorded. The data were interpolated to a rectangular grid, with a spacing of 25 m x 25 m.

Hydraulic and sedimentary conditions

Sandwaves about 5 m high are the most prominent morphological features in this area. The seabed consists of well-sorted sand with a mean diameter of 350-400 mm [*McCave*, 1971]. The mean water depth in the area ranges from 45 m in the south-west to 35 m in the east. The maximum tidal velocity at the bed is 0.75 m/s. The tidal ellipse is elongated, with the principal axis oriented SW-NE, 30^0 from the North

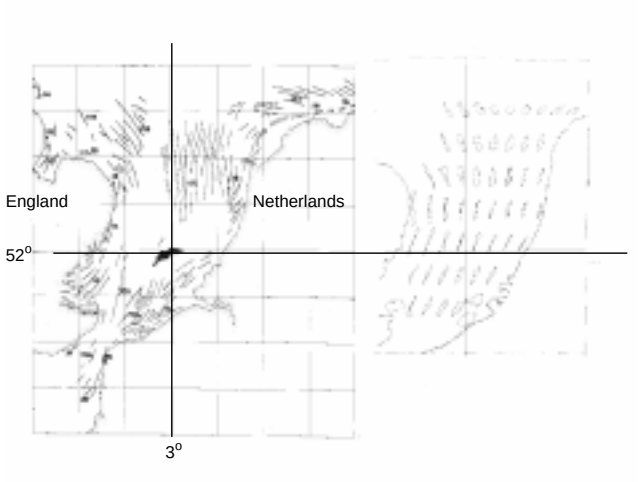

Figure 1. Left: Presence of tidal sandbanks according to [*Dyer and Huntley,* 1999]. The area studied in this paper is coloured black. Right: The near bed tidal ellipses in the North Sea according to [*McCave,* 1971].

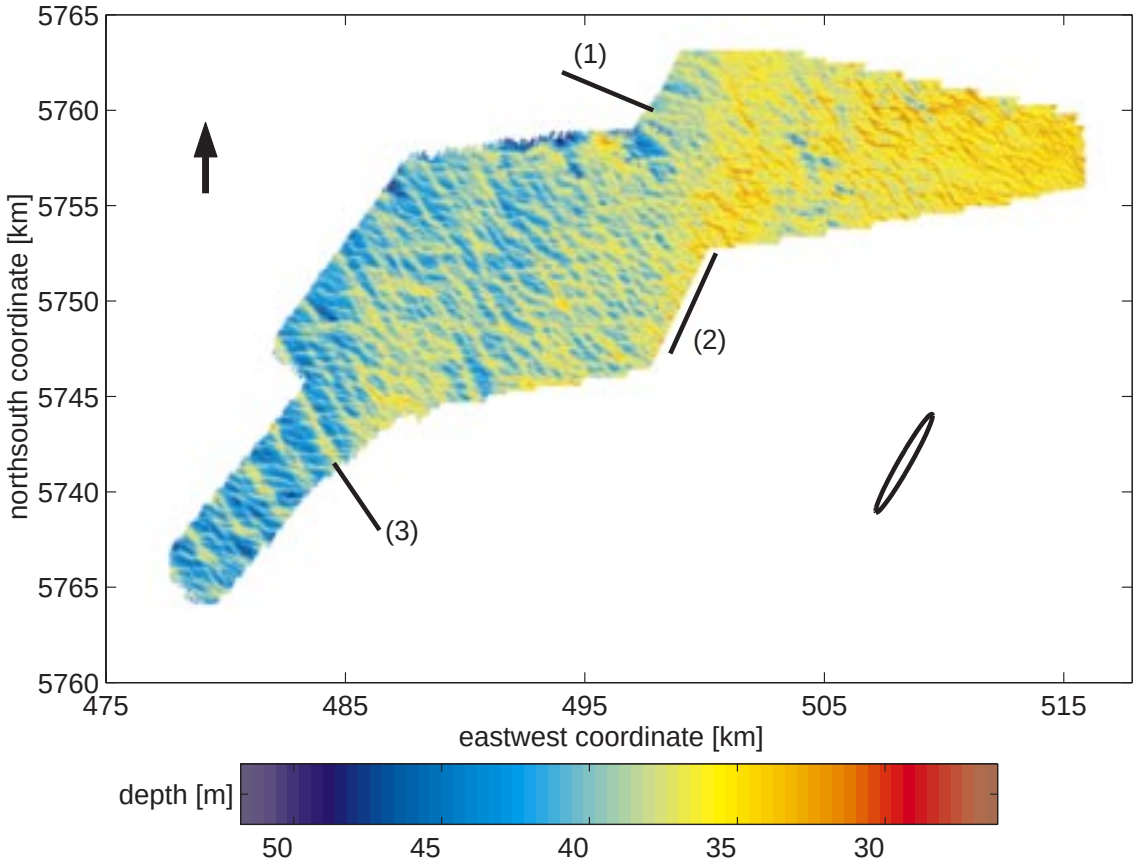

Figure 2. The measured bathymetry. There are three types of bed waves visible. The three lines indicate their crests. The arrow points North, while the ellips gives the principal tidal direction.

(Figure 1). There is a small NE-bound residual current.

Measurements revealing a new bedform

The measured bathymetry (Figure 2) is rather complex, but upon closer inspection, three types of bed waves can be distinguished (Table 1).

The shortest mode visible is the sandwave, around 600 m long with amplitude of about 5 m. The crests, though sinusoidal in planform, are about perpendicular to the principal axis of the tidal current ellipse. This is in line with the findings from linear stability analyses for tide-dominated flow [*Hulscher*, 1996].

The longest mode can be identified as low-amplitude tidal sandbanks, approximately 5 km long with an amplitude of about 1 m. Their crests are straight and rotated about 20^o counter clockwise with respect to the principal tidal axis. Tidal sandbanks have not been identified in this area before (Figure 1) [*Dyer and Huntley*, 1999; *Van Alphen and Damoiseaux*, 1989], probably due to their small height. In the echo sounding records on which the map in figure 1 is based, the more pronounced sandwaves tend to dominate all other modes.

Next to the sandwaves and the tidal sandbanks, a third mode is found, which is most energetic in the southwest of the survey area. This mode is very regular, with a wavelength of 1.6 km, an amplitude of about 5 m and a crest angle of about 60^o counter-clockwise with the principal tidal axis. Thus, both wavelength and orientation differ significantly from those of sandwaves and tidal sandbanks. This pattern can be classified neither as tidal sandbanks, nor as sandwaves.

The classification is based on the generation mechanism. The generation mechanism of sandwaves is related to their

Table 1. Characteristics of the observed bedwaves.

	wavelength $[m]$	angle with tide $[^o]$
sandwaves	550	70-90
long bedwaves	1600	50-60
tidal sandbanks	5000	0-30

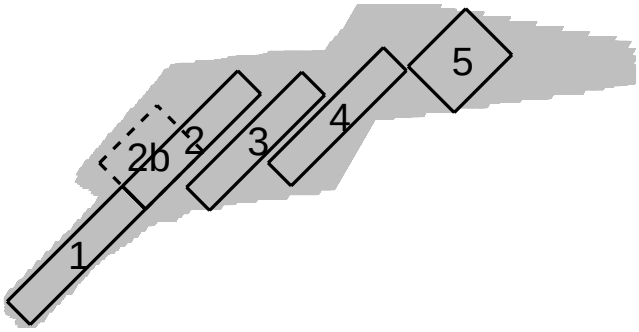

Figure 3. The measured area is divided into six parts.

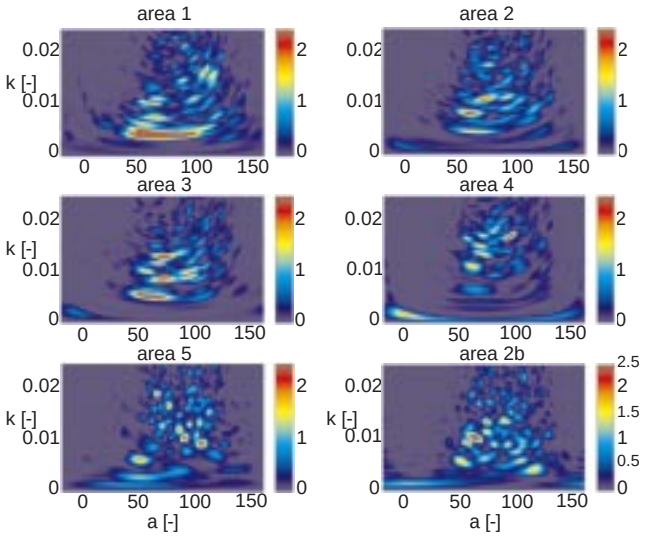

Figure 4. Power spectra scaled by the wavelength, in six parts of the measured bathymetry. κ denotes the wave number, α the counter-clockwise angle between the crests of the waves and the principal tidal direction.

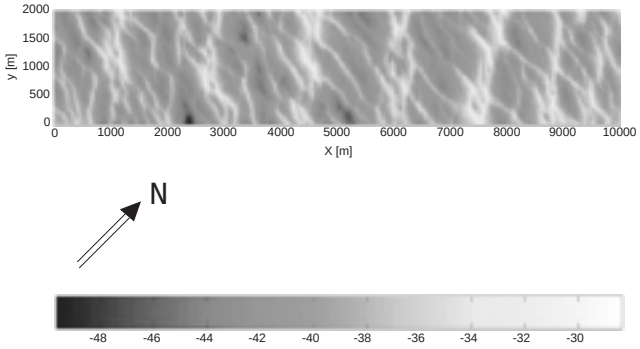

Figure 5. The bathymetry of the south-west par of the area. The mean depth is 39 m. The sandwaves are distorted by interference with the large waves.

effect on the vertical structure of the tidal flow [*Komarova and Hulscher*, 2000; *Hulscher*, 1996]. Tidal sandbanks are generated through their effect on the tidal current pattern in the horizontal [*Hulscher*, 1996; *Huthnance*, 1982]. The new pattern co-exists with sandwaves and tidal sandbanks, but has different characteristics. Therefore, this pattern can not be related to either vertical or horizontal perturbations of the tidal motion, and should be classified separately. To our knowledge, literature has not reported this third pattern before. We will refer to it as long bedwaves.

Spectral analysis

Six parts of equal area are selected in the domain (figure 3), to analyse the spectrum. Thus, we can explain the spatial variation in the measured bed pattern.

In the spectra (figure 4), there is a concentration of energy in the wavenumber band around 0.0015, corresponding with a wavelength of about 5 km. This signal is the most visible in parts 4 and 5, but it is present in the other spectra as well. Clearly, these are tidal sandbanks, although their orientation is not very distinct. From parts 2b and 5, one can observe that the angle between the crests and the principal tidal axis is somewhere between 0 and 30 degrees.

In all parts, distinct spectral peaks appear in the wave number range of the long bedwaves. The wave number varies from 0.004 (wavelength 1.6 km) in part 1 to 0.006 (wavelength 1 km) in part 5. The crests are directed 60^o counter-clockwise with respect to the principal tidal axis). The energy of the long bedwaves varies a lot over the area. The waves are distinct in part 1 and 3 (where the energy of the tidal sandbanks is low) but less so in other parts. Higher harmonics (wavelength 800 m and 400 m) are visible, indicating asymmetry of the long bedwaves.

For two reasons, the sandwave mode is not easy to identify in the spectral plots. First, the wavelengths of the three patterns differ only by a factor 3. Hence, interference effects occur: the presence of the long bedwaves effects the sandwaves. On the crest of the long bedwaves, the two modes are almost parallel, in the troughs; there is a clear difference in orientation between them. In the troughs of the long bedwaves, the sandwaves are longer than on the crests. Second, the sandwaves are sinusoidal in planform. (Figure 5) shows these effects in the southwestern part of the survey area.

Due to these effects, the sandwaves appear in the spectra as a cloud of small peaks. In part 5, where the long bedwaves are the least pronounced, there is a cloud of peaks around wavenumber 0.01 (wavelength 600 m) and angle 90^o (crests perpendicular to the main tidal axis). In part 4 the peak is found around wavenumber 0.015 (wavelength 400 m), at an angle of 70^o (i.e. rotated towards the crests of the long bedwaves). In part 3, there is a clear peak at angle 60^o and wavenumber 0.013 and a less pronounced cloud around 90^o and wavenumber 0.01. In parts 1 and 2, where the long bedwaves are more pronounced, one cannot identify any clear wavenumber or angles.

Part 2 and 2b cover almost the same area, and the differences in the spectra are limited. In 2b, the direction estimate is more precise; the wavelength estimate is less precise. Within bounds, the dimensions of the parts chosen do not affect the interpretation of the spectra.

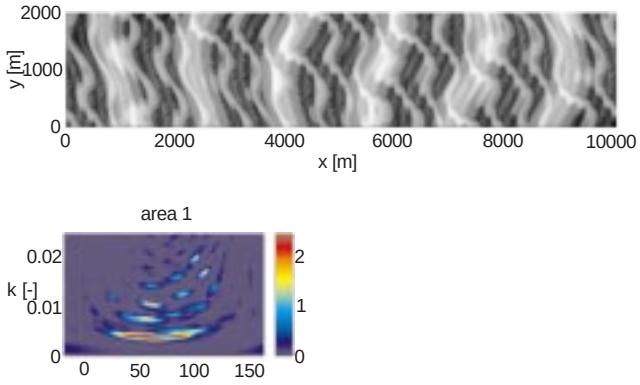

Figure 6. Top: Bathymetry representation based on sandwaves with a sinusoidal crest, superimposed on long bedwaves and tidal sandbanks. The pattern has the main characteristics of the bathymetry of part 1. Bottom: Power spectrum, scaled by the wavelength of the bathymetry representation.

Wave patterns distorted by interference

Although the pattern in figure 2 is complex, the spectral analysis shows it to be composed of only three distinct periodic patterns. We assume that interference is partly responsible for the complex patterns. To test this hypothesis, a simple data representation is built to reproduce the bathymetry in part 1 (See figure 3).

Sandwaves (wavelength 500 m, height 4 m) with crests with a sinusoidal planform, are superimposed on long bedwaves (wavelength 1.6 km, height 5 m) and tidal sandbanks (wavelength 5 km, height 1.5 m). To have interference, both the wavelength and the amplitude of the waves depend linearly on the local water depth, taking all waves with higher wavelength into account. Thus, the tidal sandbanks distort the long bedwaves and the sandwaves, while the long bedwaves distort the sandwaves.

Figure 6 shows the resulting pattern and spectrum. The model reproduces the characteristics well. Near the crests of the long bedwaves, the sandwave crests are rotated in the direction of the crests of the former. The wavelength of the sandwaves is longer in the troughs and shorter at the crests of the long bedwaves. The spectrum resembles the spectrum of part 1 (figure 4). The long bedwave mode is dominant, while a cloud of peaks around wavenumber 0.014, angle 90^o represents the sandwaves. Although included in the data representation, the tidal sandbank mode is almost invisible in the spectrum. However, their existence does distort the long bedwave mode.

Radar observations

This is not the first time that long bed waves have been observed. In 1998, similar patterns were found about 100 km south of the Noordhinder area. Using satellite born Synthetic Aperture Radar, both sandbanks and sandwaves were recorded. *Alpers* [1984] show that SAR images of the water surface can be analysed to estimate the bathymetry. *Vogelzang* [1997] show that one can measure sandwaves in this way.

However, both the wavelength and the orientation of the predominant sandwave mode were not as expected. The crests were rotated 60^o counter-clockwise, instead of 90^o. The wavelength was about 3 times the theoretical value. At the time, these differences were attributed to the limitations of the measuring system. After the above analysis however, this predominant mode appears to correspond with the long bedwaves.

Conclusions and discussion

High-resolution bathymetric monitoring in the Noordhinder area, in the Southern Bight of the North Sea, has revealed a complex bedform pattern. This pattern can be decomposed into three basic harmonic modes. Interference causes part of the complexity. Two modes, sandwaves and tidal sandbanks, are well known and have been explained from basic physical principles. The third mode has never been identified before.

It is unclear which mechanisms result in this mode. We think it is not a free instability generated by tide-bed interactions, since the instabilities found by *Hulscher* [1996] and Komarova and Newell [2000] differ in wavelength and orientation. It may be related to the spatial variation of sandwave amplitudes, whose non-linear interactions lead to a longer mode [*Komarova and Newell*, 2000]. This study, that ignores the Coriolis force, shows the existence of a longer bed mode, but not its orientation.

Acknowledgments. We would like to thank S. Bicknese of Rijkswaterstaat, the Netherlands Ministry of Transport, Public Works and Water Management, who made the data available and I. van Middelkoop and Argoss B.V. for the assessment of the SAR data of sandwaves. The work presented in this paper is supported by the Netherlands Organisation for Scientific Research (NWO) and by the Technology Foundation STW, applied science division of NWO and the technology programme of the Ministry of Economic Affairs.

References

Alpers, W., and I. Hennings, A theory of the imaging mechanism of underwater bottom topography by real and synthetic aperture radar, J. of Geophysical Res., *89* , 10529-10546, 1984.

Dyer, K.R. and D.A. Huntley, The origin, classification and modelling of sand banks and ridges, Continental Shelf Res., *19*, 1285-1330, 1999.

Hulscher, S.J.M.H., Tidal-induced Large-scale Regular Bed form patterns in a three-dimensional shallow water model, J. of Geophysical Res., *101*, C9, 20727-20744, 1996.

Huthnance, J., On one mechanism forming linear sand banks, Estuarine Coastal Shelf Sc., *14*, 461-474, 1982.

Komarova, N.L., and S.J.M.H.Hulscher, Linear instability mechanics for sand wave formation. J. of Fluid Mechanics, *413*, 219-246, 2000.

Komarova, N.L., and A.C. Newell, Nonlinear dynamics of sand banks and sand waves. J. of Fluid Mechanics, *415*, 285-312, 2000.

Van Maren, D.S., Sandwaves, A state-of-the-art review and bibliography. Report Ministry of Transport, Public Works and Water Management, North Sea Directorate, Rijswijk, the Netherlands, 1998.

McCave, N., sandwaves in the North Sea off the coast of Holland, Marine Geology, *10* , 199-225, 1971.

Meijdam, L., and P.J.M. Lapidaire, Sandwaves, upheaval buckling challenge North Sea project, Pipeline & Gas Industry, *78*, 31-38, 1995.

Off, T., Rhythmic linear sand bodies caused by tidal currents. Bulletin of the American Assoc. of Petroleum Geologists, *47*, 2, 324-341, 1963.

Pattiaratchi, C. and Collins, M., 1987. Mechanisms for linear tidal sandbank formation and maintenance in relation to dynamical oceanographic observations, Progress in Oceanography, 19, 117-176.

Trentesaux, A., A. Stolk and S. Bern, Sedimentology and stratigraphy of a tidal sand bank in the southern North Sea, Marine Geology, *159*, 253-272, 1999.

Van Alphen, J. and M. Damoiseaux, A geomorphological map of the Dutch shoreface and adjacent part of the continental shelf, Geologie en Mijnbouw, *68*, 433-443, 1989.

Vogelzang, J., G.J. Wensink, C.J. Calkoen and M.W.A. van der Kooij, Mapping submarine sandwaves with multiband imaging radar: 2. Experimental results and model comparison, J. of Geophysical Res., *102*, C1, 1183-1192, 1997.

H.J. de Vriend, S.J.M.H. Hulscher, M.A.F. Knaapen, Dep. of Civil Engineering, University of Twente, P.O.box 217, 7500 AE, Enschede, the Netherlands. e-mail: H.J.deVriend@sms.utwente.nl; S.J.M.H.Hulscher@sms.utwente.nl; M.A.F.Knaapen@sms.utwente.nl

A. Stolk, Netherlands Ministry of Transport, Public Works and Water Management, North Sea Directorate, P.O.box 5087, 2280 HV Rijswijk, the Netherlands. e-mail: A.Stolk@DNZ.RWS.MINVENW.NL

(Received July 6, 2000; revised October 16, 2000;
accepted December 27, 2000.)